JPE 9-3-2

Design of an Adaptive Backstepping Controller for Doubly-Fed Induction Machine Drives

Behzad Mirzaeian Dehkordi†, Amir Farrokh Payam*, Mohammad Naser Hashemnia*, and Seung-Ki Sul**

†Department of Electrical Engineering, Faculty of Engineering, University of Isfahan, Isfahan, Iran
*Faculty of Electrical and Computer Engineering, University of Tehran, Iran
**School of Electrical Engineering, Seoul National University, Korea

ABSTRACT

In this paper, a nonlinear controller is proposed for Doubly-Fed Induction Machine (DFIM) drives. The nonlinear controller is designed based on an adaptive backstepping control technique, using a fifth order model of an induction machine in the synchronous d & q axis rotating reference frame, whose d axis coincides with the space voltage vector of the main AC supply, and using the rotor current and stator flux components as state variables. The nonlinear controller can perfectly track the torque reference signal measured in the stator terminals under the condition of unity power factor regulation, in spite of the stator and rotor resistance variations. In order to make the drive system capable of operating in the motoring and generating modes below and above the synchronous speed, two level Space-Vector PWM (SV-PWM) back-to-back voltage source inverters are employed in the rotor circuit. It is confirmed through computer simulation results that the proposed control approach is effective and valid.

Keywords: Adaptive backstepping, Doubly-fed induction machine, Unity power factor

1. Introduction

In a Doubly-Fed Induction Machine (DFIM), since the air gap slip power can be easily controlled by its rotor circuit converter, the machine drive can operate as a generator and a motor below and above the synchronous speed [1]. Fig.1 shows a general block diagram of a DFIM system where its operation modes are described in Table 1 [2]. The vector control of a DFIM is an attractive solution for restricted speed range drives, especially wind power generation applications, where the mechanical input is varying and unpredictable [3-5]. The principal theory of a vector controlled DFIM drive has been described in [4] and [5]. The induction machine is driven in the vector control at the stator flux oriented reference frame, while the active and reactive powers injected to the stator circuit can be controlled independently. In the design of the controller in [4] and [5], the voltage drop across the stator leakage impedance had been neglected. Having made this assumption, a steady-state error is expected. In addition, in the field oriented control method, the decoupled relationship is obtained by means of a proper selection of

Manuscript received August, 8, 2008; revised February, 9, 2009
†Corresponding Author: mirzaeian@eng.ui.ac.ir
Tel: +98 311 793 4045, Fax: +98 311 793 2771, Univ. of Isfahan.
*Faculty of Electrical and Computer Engineering, Univ. of Tehran, Tehran, Iran
**School of Electrical Engineering, Seoul Nat'l Univ., Korea

state coordinates (in the case of a DFIM drive, a stator flux oriented reference frame), under the hypothesis that the oriented flux is kept constant. Therefore, the rotor speed or motor generated torque in this asymptotically decoupled relationship shows that the stator flux and rotor speed are only linearly related to the torque current component under the steady-state condition when the stator flux ideally becomes a constant value. This means the field oriented method is basically not a tracking control method. In addition, there is no guarantee that by this method the drive system can preserve its stability in the transient-state. To solve these problems, a few researchers have tried to apply nonlinear control methods to a DFIM drive system[6, 7]. In [6] and [7], a backstepping torque tracking controller was presented for a DFIM drive on the basis of unity power factor operation (measured in the stator terminals), and the performance of the drive system was evaluated only for the generating mode of operation above the synchronous speed and with nominal parameters. The main purpose of this paper is to continue the research work described in [6] and to extend the performance evaluation of the DFIM drive system to the motoring and generating modes of operation below and above the synchronous speed. Also, it can be proved that the proposed controller is robust against rotor and stator resistance uncertainties. A full proof for the convergence of states is verified together with stability for the quantity estimations. It will be shown that the proposed controller is capable of perfectly tracking the torque reference commands with unity power factor regulation in spite of the machine resistance variations and external load torque disturbances.

Moreover, in order to make the DFIM drive system capable of operating in motoring and generating modes of operation, below and above the synchronous speed, two level Space Vector-PWM (SV-PWM) back-to-back Voltage-Source Inverters (VSI) are employed in the rotor circuit. In this control scheme, the rotor DC-link voltage is maintained as constant on the basis of the input-output feedback linearization technique.

Finally, the drive system performance is demonstrated by simulation results. Also, by comparing the results from the conventional Proportional and Integral (PI) controller and those from the backstepping controller, the effectiveness of the proposed controller is verified.

Table 1 DFIM system modes of operation

Speed\Mode	Generating	Motoring
Sub-Synchronous	$P_S<0\ P_r>0$	$P_S>0\ P_r<0$
Super-Synchronous	$P_S<0\ P_r<0$	$P_S>0\ P_r>0$

2. Doubly-Fed Induction Machine Model

Under the assumption of linear magnetic circuits and balanced operating conditions, the equivalent two-phase model of the symmetrical DFIM with stator connected to line, represented in the stator voltage d-q reference frame is,

$$\begin{aligned}
\frac{di_{dr}}{dt} &= -\gamma_2 i_{dr} + \omega_2 i_{qr} + \beta\alpha_1\psi_{ds} - \beta\omega\psi_{qs} - \beta U + \frac{1}{L_\sigma}u_{dr}\\
\frac{di_{qr}}{dt} &= -\gamma_2 i_{qr} - \omega_2 i_{dr} + \beta\alpha_1\psi_{qs} + \beta\omega\psi_{ds} + \frac{1}{L_\sigma}u_{qr}\\
\frac{d\psi_{ds}}{dt} &= \alpha_1 L_m i_{dr} - \alpha_1\psi_{ds} + \omega_0\psi_{qs} + U\\
\frac{d\psi_{qs}}{dt} &= \alpha_1 L_m i_{qr} - \alpha_1\psi_{qs} - \omega_0\psi_{ds}\\
\frac{d\omega}{dt} &= \frac{1}{J}[\mu(\psi_{qs} i_{dr} - \psi_{ds} i_{qr}) - T_L]
\end{aligned} \tag{1}$$

where i_r, ψ_s, U, u_r, R_r and L_r denote rotor current, stator flux linkage, stator terminal voltage, rotor terminal voltage, resistance and inductance, respectively. The subscripts s and r stand for stator and rotor while the subscripts d and q stand for the vector component with respect to the stator voltage reference frame. ω, denotes the rotor electrical speed and L_m is the mutual inductance.

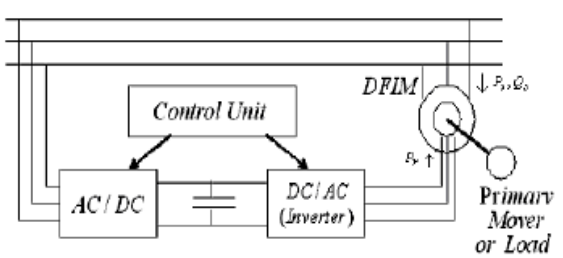

Fig. 1. Electrical circuit configuration of DFIM system.

$\omega_2 = \omega_0 - \omega$, is the slip speed and $L_\sigma = L_r(1-(\frac{L_m^{\ 2}}{L_r L_s}))$, is the redefined leakage inductance. Also,

$$\alpha_1 = \frac{R_s}{L_s}, \beta = \frac{L_m}{L_\sigma L_s}, \gamma_2 = (\alpha_1 \beta L_m + \frac{R_r}{L_\sigma}), \mu = \frac{3PL_m}{2L_s} \quad (2)$$

where P is the number of poles.

The torque generated by DFIM can be expressed in terms of rotor currents and stator flux linkage as,

$$T_e = \mu(\psi_{qs} i_{dr} - \psi_{ds} i_{qr}) \quad (3)$$

The mechanical dynamic equation is given by,

$$J\frac{d\omega_m}{dt} + B\omega_m + T_L = T_e \quad (4)$$

where J and B denote the moment of inertia of the motor and viscous friction coefficient, respectively, T_L is the external load and ω_m is the rotor mechanical speed ($\omega = (\frac{P}{2})\omega_m$).

To achieve steady-state unity power factor on the stator side of the machine, the d-axis stator flux should asymptotically approach zero, i.e.,[6], [7].

$$\lim_{t\to\infty} \psi_{ds} = 0 \quad (5)$$

Equation (5) reveals that, under unity power factor operation, stator voltage orientation means stator flux orientation too. As no measurement or calculation has been done to achieve stator flux orientation, the applied nonlinear control method can also be called, "indirect stator flux orientation" [7]. Perfect torque tracking is the other considered specification, in particular, the torque reference, which is assumed to be bounded together with its first and second derivatives. At this point, the two outputs of the DFIM to be controlled can be defined as,

$$y = \begin{pmatrix} T_e \\ \psi_{ds} \end{pmatrix} \quad (6)$$

Control input is the two-dimensional rotor voltage vector $u_r = [u_{dr}, u_{qr}]^T$. In the motor operation of this drive for the speed control objective, a PI controller is used as the speed controller. The following control task is then formulated. Using the measured variables, rotor voltages are designed in order to perform asymptotic torque tracking, a unity power factor is achieved during steady state, while guaranteeing internal stability and this implies the following:

$$\lim_{t\to\infty} \tilde{T} = 0, \quad \lim_{t\to\infty} \psi_{ds} = 0 \quad (7)$$

where the tracking error is defined as, $\tilde{T} = T_e - T^*$.

3. Adaptive Backstepping Torque-Flux Controller Design

The design procedure is performed in two steps. Firstly, the flux-torque control algorithm is developed to design rotor current references. Secondly, based on rotor current references, according to the rotor voltages, in order to perform asymptotic torque tracking, a unity power factor is achieved during steady state.

Considering the following:

$$\begin{aligned} T_e &= \mu(\psi_{qs} i_{dr} - \psi_{ds} i_{qr}) \\ \frac{d\psi_{ds}}{dt} &= \alpha_1 L_m i_{dr} - \alpha_1 \psi_{ds} + \omega_0 \psi_{qs} + U \\ \frac{d\psi_{qs}}{dt} &= \alpha_1 L_m i_{qr} - \alpha_1 \psi_{qs} - \omega_0 \psi_{ds} \end{aligned} \quad (8)$$

The stator flux errors are defined as,

$$\tilde{\psi}_{ds} = \psi_{ds}, \tilde{\psi}_{qs} = \psi_{qs} - \psi^*, \tilde{\alpha}_1 = \hat{\alpha}_1 - \alpha_1 \quad (9)$$

where $\psi^* \neq 0$ is the reference for the modulus of the flux vector and $\hat{\alpha}_1$ is the estimated value of α_1 which is calculated by (22) (proof will be given below). Using error definitions, equation (8) can be rewritten as,

$$\begin{aligned} \tilde{T} &= \mu\left((\tilde{\psi}_{qs} + \psi^*) i_{dr} - \tilde{\psi}_{ds} i_{qr}\right) \\ \dot{\tilde{\psi}}_{ds} &= -\alpha_1 \tilde{\psi}_{ds} + \omega_0 (\tilde{\psi}_{qs} + \psi^*) + \alpha_1 L_m i_{dr} + U \\ \dot{\tilde{\psi}}_{qs} &= -\omega_0 \tilde{\psi}_{ds} - \alpha_1 (\tilde{\psi}_{qs} + \psi^*) + \alpha_1 L_m i_{qr} - \dot{\psi}^* \end{aligned} \quad (10)$$

Defining the following:

-Torque control algorithm: $i_{dr} = \dfrac{T^*}{\mu\psi^*}$ (11)

-Flux reference for the desired trajectory given by,

$$\omega_0\psi^* + \hat{\alpha}_1 L_m \frac{T^*}{\mu\psi^*} + U = 0 \quad (12)$$

-Flux control algorithm:

$$i_{qr} = \frac{1}{\hat{\alpha}_1 L_m}(\hat{\alpha}_1\psi^* + \dot{\psi}^*) \quad (13)$$

Error dynamics (10) become,

$$\begin{aligned}
\tilde{T} &= \mu\left(\tilde{\psi}_{qs} i_{dr} - \tilde{\psi}_{ds} i_{qr}\right) \\
\dot{\tilde{\psi}}_{ds} &= -\alpha_1\tilde{\psi}_{ds} + \omega_0\tilde{\psi}_{qs} - \tilde{\alpha}_1 L_m i_{dr} \\
\dot{\tilde{\psi}}_{qs} &= -\omega_0\tilde{\psi}_{ds} - \alpha_1\tilde{\psi}_{qs} - \frac{\tilde{\alpha}_1}{\hat{\alpha}_1}\dot{\psi}^*
\end{aligned} \quad (14)$$

Defining the rotor current tracking error as,

$$\tilde{i}_{dr} = i_{dr} - {i_{dr}}^*, \tilde{i}_{qr} = i_{qr} - {i_{qr}}^* \quad (15)$$

The stator flux, rotor current error dynamics can be computed from (14) and (1) as,

$$\begin{aligned}
\dot{\tilde{\psi}}_{ds} &= -\alpha_1\tilde{\psi}_{ds} + \omega_0\tilde{\psi}_{qs} + \alpha_1 L_m\tilde{i}_{dr} - \tilde{\alpha}_1 L_m i_{dr}^* \\
\dot{\tilde{\psi}}_{qs} &= -\alpha_1\tilde{\psi}_{qs} - \omega_0\tilde{\psi}_{ds} + \alpha_1 L_m\tilde{i}_{qr} - \frac{\tilde{\alpha}_1}{\hat{\alpha}_1}\dot{\psi}^* \\
\dot{\tilde{i}}_{dr} &= -\gamma_2\tilde{i}_{dr} + \omega_2\tilde{i}_{qr} + \beta\alpha_1\tilde{\psi}_{ds} - \beta\omega\tilde{\psi}_{qs} - \gamma_2 i_{dr}^* + \omega_2 i_{qr}^* - \ldots \\
&\quad \beta\omega\psi^* - \beta U + \frac{1}{L_\sigma}u_{dr} - \dot{i}_{dr} \\
\dot{\tilde{i}}_{qr} &= -\gamma_2\tilde{i}_{qr} - \omega_2\tilde{i}_{dr} + \beta\alpha_1\tilde{\psi}_{qs} + \beta\omega\tilde{\psi}_{ds} - \gamma_2 i_{qr}^* - \omega_2 i_{dr}^* + \beta\alpha_1\psi^* + \frac{1}{L_\sigma}u_{qr} - \dot{i}_{qr}
\end{aligned} \quad (16)$$

The rotor voltages should be designed to achieve asymptotic rotor current tracking and to guarantee global asymptotic stability for the full system. The current control is selected as,

$$u_{dr} = L_\sigma[\hat{\gamma}_2 i_{dr}^* - \omega_2 i_{qr}^* + \beta\omega\psi^* + \beta U + \dot{i}_{dr}^* - k_i\tilde{i}_{dr} - k_{ii}x_d]$$

$$u_{qr} = L_\sigma[\hat{\gamma}_2 i_{qr}^* + \omega_2 i_{dr}^* - \beta\hat{\alpha}_1\psi^* + \dot{i}_{qr}^* - k_i\tilde{i}_{qr} - k_{ii}x_q] \quad (17)$$

In this equation x_d, x_q are variables to construct the integral section of current controller and $k_i > 0, k_{ii} > 0$ are the proportional and integral gains of the current controller, which must be selected to stabilize the system. Substituting (16) into (17), the resulting system error dynamics become,

$$\begin{aligned}
\dot{\tilde{\psi}}_{ds} &= -\alpha_1\tilde{\psi}_{ds} + \omega_0\tilde{\psi}_{qs} + \alpha_1 L_m\tilde{i}_{dr} - \tilde{\alpha}_1 L_m i_{dr}^* \\
\dot{\tilde{\psi}}_{qs} &= -\alpha_1\tilde{\psi}_{qs} - \omega_0\tilde{\psi}_{ds} + \alpha_1 L_m\tilde{i}_{qr} - \frac{\tilde{\alpha}_1}{\hat{\alpha}_1}\dot{\psi}^* \\
\dot{\tilde{i}}_{dr} &= -(\gamma_2 + k_i)\tilde{i}_{dr} + \tilde{\gamma}_2 i_{dr}^* + \omega_2\tilde{i}_{qr} - k_{ii}x_d + \beta\alpha_1\tilde{\psi}_{ds} - \beta\omega\tilde{\psi}_{qs} \\
\dot{\tilde{i}}_{qr} &= -(\gamma_2 + k_i)\tilde{i}_{qr} + \tilde{\gamma}_2 i_{qr}^* - \omega_2\tilde{i}_{dr} - k_{ii}x_q + \beta\alpha_1\tilde{\psi}_{qs} - \beta\tilde{\alpha}_1\psi^* + \beta\omega\tilde{\psi}_{ds} \\
\dot{x}_d &= \tilde{i}_{dr} \\
\dot{x}_q &= \tilde{i}_{qr}
\end{aligned} \quad (18)$$

For this extent, consider the positive-definite function as,

$$V = \frac{1}{2}\left((\tilde{\psi}_{ds}^2 + \tilde{\psi}_{qs}^2) + \gamma_i(\tilde{i}_{dr}^2 + \tilde{i}_{qr}^2) + \gamma_{ii}(x_d^2 + x_q^2) + \frac{1}{\gamma_\alpha}\tilde{\alpha}_1^2 + \frac{1}{\gamma_\beta}\tilde{\gamma}_2^2\right) \quad (19)$$

where γ_i, γ_{ii} are arbitrary positive parameters, when it is selected, $\gamma_{ii} = \gamma_i k_{ii}$. The time-derivative of V, along the trajectories of (18) is,

$$\begin{aligned}
\dot{V} &= -\alpha_1(\tilde{\psi}_{ds}^2 + \tilde{\psi}_{qs}^2) + \alpha_1(\gamma_i\beta + L_m)(\tilde{\psi}_{ds}\tilde{i}_{dr} + \tilde{\psi}_{qs}\tilde{i}_{qr}) - \ldots \\
&\quad \gamma_i(k_i + \gamma_2)(\tilde{i}_{dr}^2 + \tilde{i}_{qr}^2) + \gamma_i\beta\omega(\tilde{\psi}_{ds}\tilde{i}_{qr} - \tilde{\psi}_{qs}\tilde{i}_{dr}) + \ldots \\
&\quad \tilde{\alpha}_1(-L_m i_{dr}^*\tilde{\psi}_{ds} - \frac{\tilde{\psi}_{qs}\dot{\psi}^*}{\hat{\alpha}_1} - \gamma_i\beta\psi^*\tilde{i}_{qr} + \frac{1}{\gamma_\alpha}\dot{\tilde{\alpha}}_1) + \ldots \\
&\quad \tilde{\gamma}_2(\frac{1}{\gamma_\beta}\dot{\tilde{\gamma}}_2 + \gamma_i(\tilde{i}_{dr}i_{dr}^* + \tilde{i}_{qr}i_{qr}^*))
\end{aligned} \quad (20)$$

The function (20) is negative semi-definite if the following condition for the proportional gain of the current controller is satisfied (appendix),

$$k_i > \frac{1}{2\alpha_1}\left(\gamma_i\beta^2(\omega_{\max}^2 + {\alpha_1}^2) + \frac{\alpha_1^2 L_m^2 + 4k_p}{\gamma_i} + 2\alpha_1^2\beta L_m\right) \quad (21)$$

and the adaptation laws are,

$$\dot{\tilde{\alpha}}_1 = \gamma_\alpha \left(L_m i_{dr}^* \tilde{\psi}_{ds} + \frac{\tilde{\psi}_{qs} \psi^*}{\hat{\alpha}_1} + \gamma_i \beta \psi^* \tilde{i}_{qr} \right)$$
$$\dot{\tilde{\gamma}}_2 = -\gamma_\beta \gamma_i \left(\tilde{i}_{dr} i_{dr}^* + \tilde{i}_{qr} i_{qr}^* \right) \quad (22)$$

where k_p is arbitrary, but greater than 0, and $\omega_{\max}$ is the maximum value for the system. From (19)-(22) it can be concluded that, $x = [\tilde{i}_{dr}, \tilde{i}_{qr}, \tilde{\psi}_{ds}, \tilde{\psi}_{qs}, x_d, x_q]^T$ is bounded, also the reference flux is calculated from (12) simultaneously with the equations (19)-(22). From boundless torque and its first and second derivatives and from direct application of Barbalat's lemma [8], it follows that,

$$\lim_{t \to \infty} x = 0 \quad (23)$$

So the stability of the control system is proved.

4. Stabilization of Rotor DC-Link Voltage

In this paper the rotor DC- link voltage is maintained as constant on the basis of the input-output feedback linearization technique. The control strategy is shown in Fig. 2, as described in [9]. Using the control method in [9], the d and q axis equations corresponding to the main AC power supply in a particular synchronous rotating reference frame with the d axis coinciding with the voltage space vector are given by:

$$\frac{di_d}{dt} = \frac{1}{L}(v_d - Ri_d + \omega_e L i_q - v_{d1})$$
$$\frac{di_q}{dt} = \frac{1}{L}(-Ri_q - \omega_e L i_d - v_{q1}) \quad (24)$$

One may note that in this reference frame, the d axis being coincident with the main space voltage vector means that $v_d = v_s$, and $v_q = 0$.

Considering i_d^*, i_q^* as reference currents, the current errors are,

$$e_1 = i_d - i_d^* \quad , \quad e_2 = i_q - i_q^* \quad (25)$$

As the result, the system error dynamics are:

$$\dot{e}_1 = \frac{v_d}{L} - \frac{R}{L} i_d + \omega_e i_q - \frac{v_{d1}}{L} - \dot{i}_d^*$$
$$\dot{e}_2 = -\frac{R}{L} i_q - \omega_e i_d - \frac{v_{q1}}{L} - \dot{i}_q^* \quad (26)$$

Defining the AC side inverter reference voltages as,

$$v_{d1} = L\left(\frac{v_d}{L} - \frac{R}{L} i_d + \omega_e i_q - \dot{i}_d^* - k e_1\right)$$
$$v_{q1} = L\left(-\frac{R}{L} i_q - \omega_e i_d - \dot{i}_q^* - k e_2\right) \quad (27)$$

Linking (26) and (27), gives:

$$\dot{e}_1 = -k e_1 \quad , \dot{e}_2 = -k e_2 \quad (28)$$

Considering a Lyapanouv function and its derivative as,

$$V = \frac{1}{2} e_1^2 + \frac{1}{2} e_2^2 \quad (29)$$

The derivative of this function becomes:

$$\dot{V} = \dot{e}_1 e_1 + \dot{e}_2 e_2 = -k(e_1^2 + e_2^2) < 0 \quad (30)$$

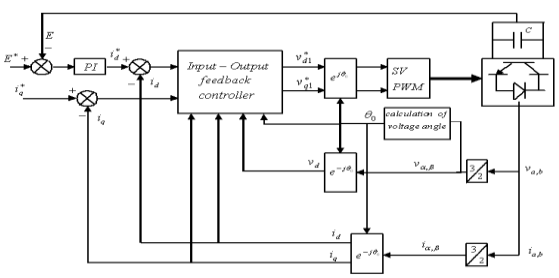

Fig. 2. DC-link voltage controller [9].

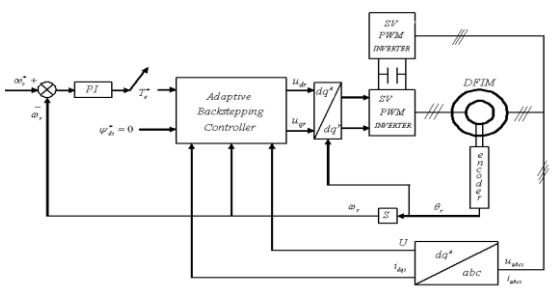

Fig. 3. Block diagram of the proposed controller.

5. Simulation Results

The overall block diagram of the proposed control approach is shown in Fig. 3. A C++ computer program was developed to model this system.

As shown in Fig.3, the SV-PWM method has been used for the switching of the two inverters in the rotor circuit. The greatest advantages of the SV-PWM method compared to conventional PWM techniques are flexibility in design and and better performance in operation plus the reduction of harmonic distortion in the system. In this program, a static Runge- Kutta fourth order method is used to solve the system equations. The effectiveness and validity of the proposed approach is tested for a three-phase 5 kW, 380 V r.m.s line-to-line voltage, six poles, 50 Hz, DFIM drive [10], by computer simulation and the results obtained by backstepping and conventional PI controller are compared.

5.1 Test one

In this test, the drive system performance in the motoring mode of operation below and above the synchronous speed with nominal parameters is simulated with the conventional PI and the proposed controller. In this case, the reference speed is increased from 0 to 250 (rad/sec) at t=0 sec and from 250 (rad/sec) to 375 (rad/sec) at t=2 sec with the load torque described as follows:

$$T_L = 30N.m \quad \text{t=0}, \quad T_L = 35N.m \quad \text{t=.9 sec},$$
$$T_L = 25N.m \quad \text{t=1.8 sec}, \quad T_L = 20N.m \quad \text{t=2.7 sec}$$

Fig. 4 shows the results obtained for the conventional PI controller. As shown, transient dynamics, especially when the motor starts, are considerable in this case. In addition, there is a large torque error when the motor speed changes from subsynchronous to super synchronous speed. Also, dynamic transients are obvious in currents and fluxes.

For the purpose of investigating motoring operation in a practical environment, another simulation test is done by adding noise and offset to the measured motor speed in the system drive. Therefore, white noise, whose magnitude is 1 r/min and 100 (micro sec) sampling times is considered as the speed noise, also a speed offset with a magnitude of 0.1 (rad/min) is assumed. The simulation results with the addition of the white noise and the offset to the measured motor speed are shown in Fig. 5 and Fig. 6 for the conventional PI controller and the adaptive backstepping controller, respectively. In this test, the drive system's performance in the motoring mode of operation below and above the synchronous speed is obtained. These results show that the conventional controller works perfectly in steady state but noise and offset effect on transients and transient errors are larger than the adaptive controller.

Comparison of the two controllers shows that the operation of the motor system under the adaptive backstepping controller is better than the conventional PI controller, especially in the transient mode. In addition, during the change in the rotor speed from below synchronous speed to above synchronous speed, in the conventional PI controller, there is a considerable transient error in torque while in the proposed controller the error is reduced significantly.

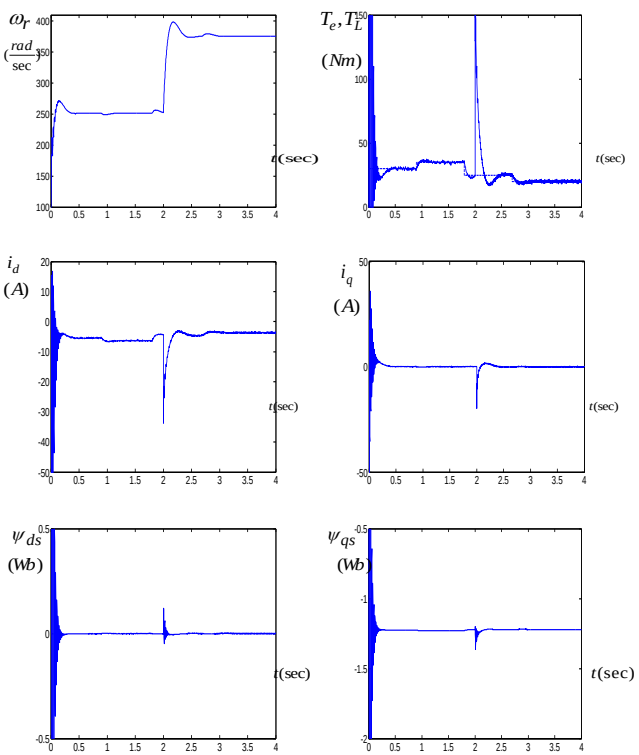

Fig. 4. Simulation results for motoring mode of operation with the conventional PI controller.

5.2 Test two

To investigate the robustness of the proposed approach, the motoring mode performance of the adaptive backstepping controller is evaluated under parameter variations and uncertainties in the presence of the noise and offset in the measured motor speed. Fig. 7 shows the drive system performance in the motoring mode of operation below and above synchronous speed.

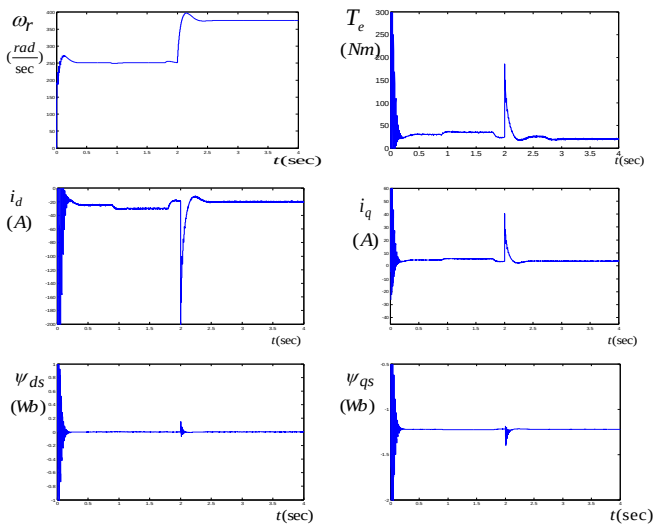

Fig. 5. Simulation results for motoring mode of operation with noise and offset using the conventional PI controller.

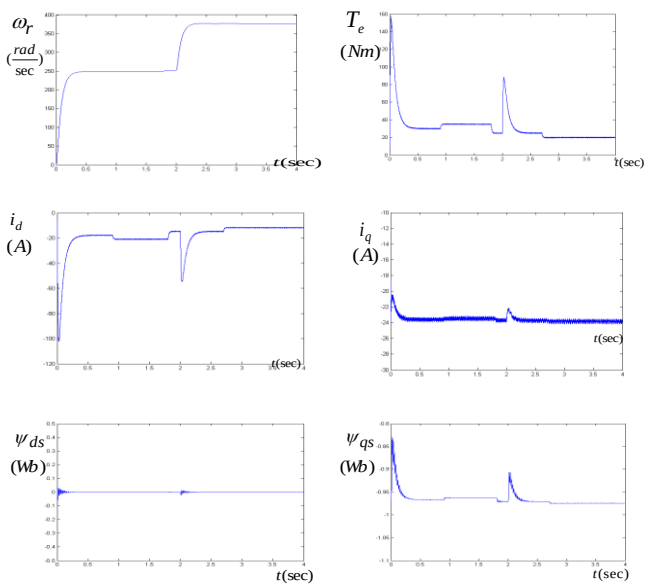

Fig. 6. Simulation results for motoring mode of operation with noise and offset using the adaptive backstepping controller.

The results are obtained with $R_r = 2R_{rn}$ and $R_s = 2R_{sn}$. In this case, to investigate the drive behavior in a practical environment, the effects of noise and offset in the measured motor speed, similar to the first test have been considered. From this figure, it can be concluded that the controller works perfectly under variations of rotor and stator resistances and in a noisy environment and the control objectives are met completely.

5.3 Test three

In the following the behavior of the generating mode of operation is studied. For this purpose, some simulations' tests, below and above the synchronous speed with and without uncertainties are considered. Fig. 8 (a) and Fig 8 (b) show the drive system performance in the generating mode of operation below the synchronous speed (275 (rad/sec)) using the conventional PI controller and the adaptive backstepping controller in a noisy environment for the motor speed (similar to the test one), respectively. These results are obtained with the nominal induction machine parameters.

As shown by these results, due to the nonlinear nature of the proposed controller, the proposed nonlinear controller reveals considerably better performance in torque tracking than the conventional PI controller. For the purpose of studying the controller performance in the generating mode of operation and under uncertainties and parameter variations, some simulation tests have been done.

Figs. 9-10 show the drive system performance in the generating mode of operation below the synchronous speed with the conventional PI control method and the method used in [4,5], respectively. These results are obtained with $R_r = 2R_{rn}$ and $R_s = 2R_{sn}$. As shown by Figs. 9-10, there are errors between torque and current references and actual values. But, in this paper, by using the proposed controller, these errors are removed and the torque and current perfectly track their references under the presence of uncertainties in the rotor and stator resistances.

Fig. 11 shows the drive system performance in the generating mode of operation below the synchronous speed using the proposed controller. The results are

obtained with $R_r = 2R_{rn}$ and $R_s = 2R_{sn}$. Oscillations occurring in the flux profile are related to the changes of the torque commands.

Now, the DFIM behavior above the synchronous speed is investigated. So, the DFIM is simulated at 380 (rad/sec). Fig. 12 shows the drive system performance in the generating mode of operation above the synchronous speed. The results are obtained with $R_r = 2R_{rn}$ and $R_s = 2R_{sn}$.

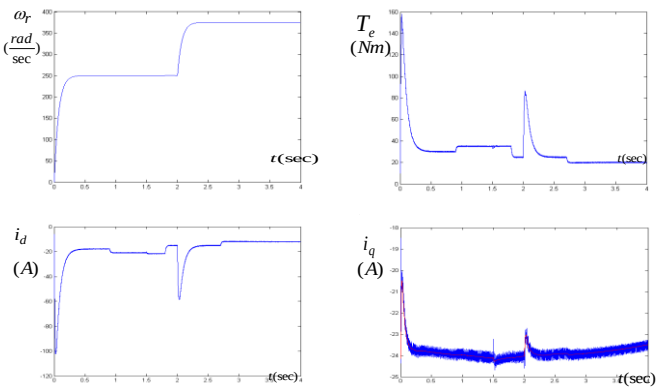

Fig. 7. Simulation results for motoring mode of operation in test two using the adaptive backstepping controller.

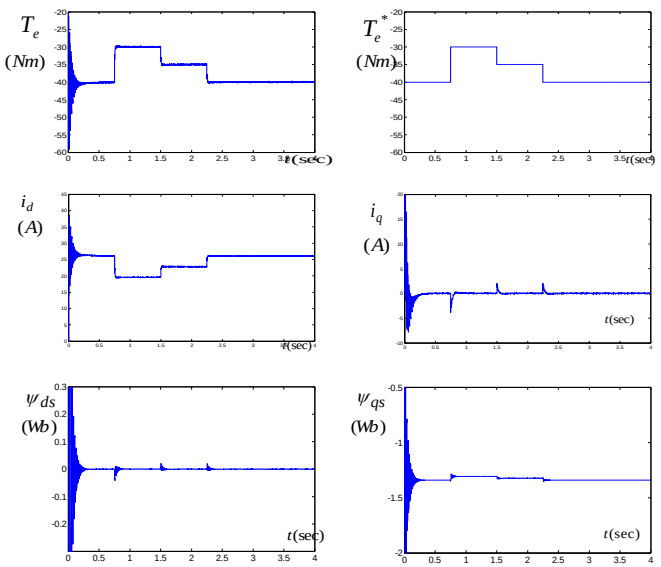

Fig. 8-a. Simulation results for subsynchronous generating mode of operation under noisy conditions using the conventional PI controller.

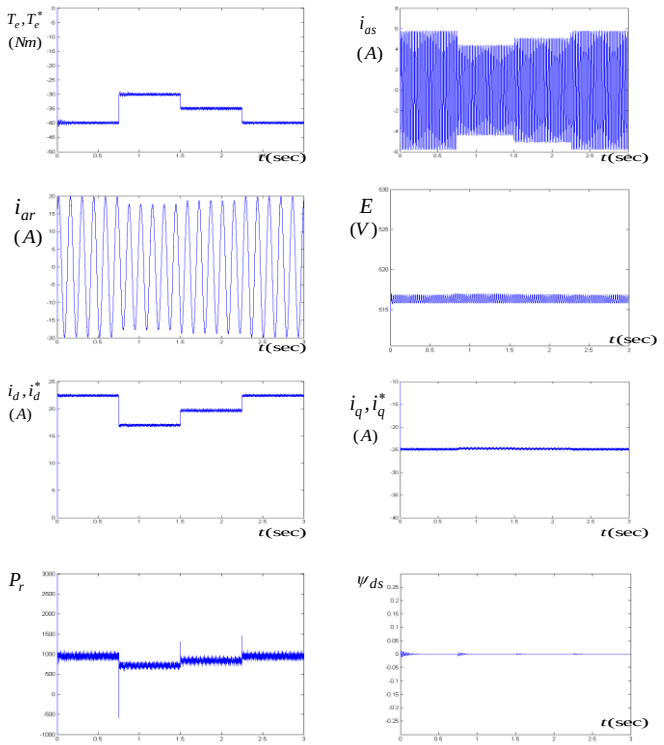

Fig. 8-b. Simulation results for generating mode below synchro nous speed under noisy conditions using the adaptive backstepping controller.

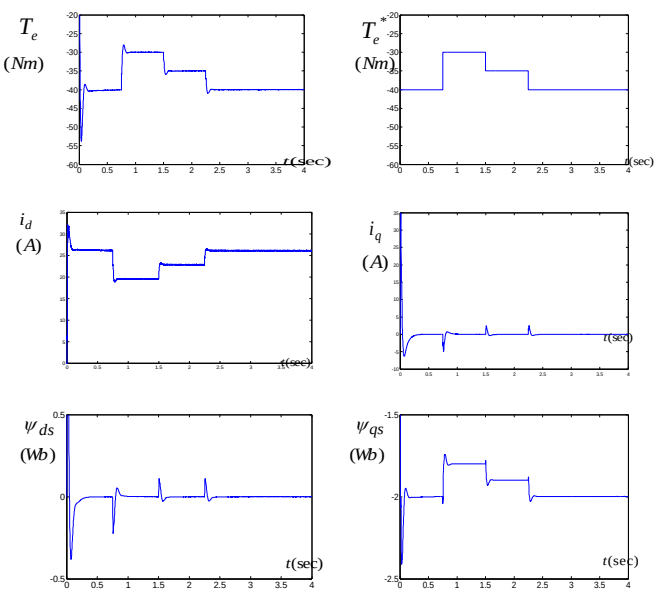

Fig. 9. Simulation results for generating mode below the synchronous speed with the conventional PI controller with $R_r = 2R_{rn}, R_s = 2R_{sn}$.

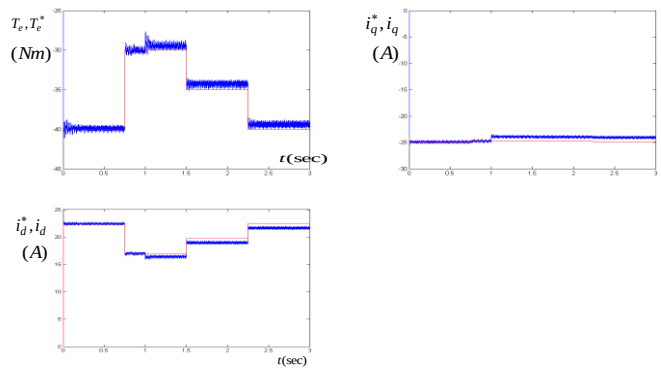

Fig. 10. Simulation results for generating mode below synchronous speed with the method used in [4,5].

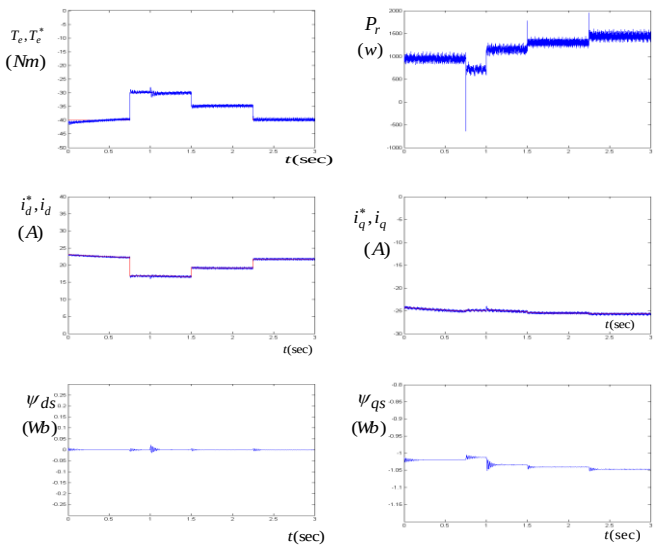

Fig. 11. Simulation results for generating mode below synchronous speed using the adaptive backstepping controller.

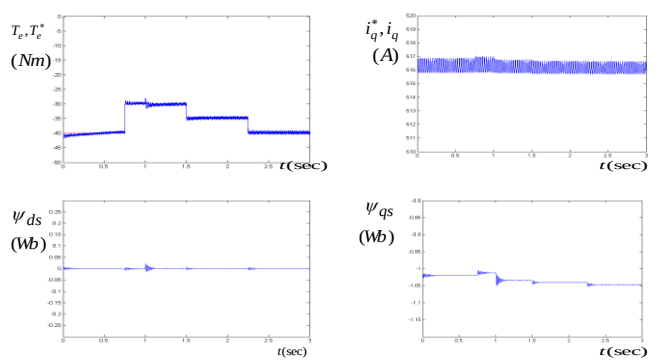

Fig. 12. Simulation results for generating mode above the synchronous speed with using the adaptive backstepping controller.

As seen from these figures, using the proposed controller, the control objective can be achieved in the presence of uncertainties and variations in the rotor and stator resistances and external load torque disturbance.

6. Conclusions

In this paper an adaptive nonlinear controller has been proposed for DFIM drives. The proposed controller is designed based on an adaptive backstepping control approach and is capable of making the torque of the DFIM follow the torque reference with the unity power factor condition in spite of stator and rotor resistance uncertainties and external load torque disturbances. The proposed control approach has been verified for both the motoring and generating modes of operation below and above the synchronous speed by simulation, using two level SV-PWM back-to-back voltage sources inverters in the rotor circuit. Furthermore, the rotor DC- link voltage is maintained as constant based on an input-output control method, using a rotating synchronous reference frame with d axis coinciding with the direction of the space voltage vector of the main AC supply. Computer simulation results confirm the validity and effectiveness of the proposed control approach.

Appendix

By considering the Lyapanouv function:

$$V = -\alpha_1\left[\frac{\tilde{\psi}_d}{\sqrt{2}} - \frac{(\gamma_i\beta + L_m)}{\sqrt{2}}\tilde{i}_d\right]^2 - \alpha_1\left[\frac{\tilde{\psi}_q}{\sqrt{2}} - \frac{(\gamma_i\beta + L_m)}{\sqrt{2}}\tilde{i}_q\right]^2 - \ldots$$
$$\left[\frac{\sqrt{\alpha_1}\tilde{\psi}_d}{\sqrt{2}} - \frac{(\gamma_i\beta\omega)}{\sqrt{2\alpha_1}}\tilde{i}_q\right]^2 - \left[\frac{\sqrt{\alpha_1}\tilde{\psi}_q}{\sqrt{2}} + \frac{(\gamma_i\beta\omega)}{\sqrt{2\alpha_1}}\tilde{i}_d\right]^2 \le 0$$

We have:

$$V = -\alpha_1\left(\tilde{\psi}_d^2 + \tilde{\psi}_q^2\right) + \left(\tilde{i}_d\tilde{\psi}_d + \tilde{i}_q\tilde{\psi}_q\right)\left[\alpha_1\gamma_i\beta + \alpha_1 L_m\right] +$$
$$\left(\tilde{\psi}_d\tilde{i}_q - \tilde{\psi}_q\tilde{i}_d\right)\left[\gamma_i\beta\omega\right] - \ldots$$
$$\left(\tilde{i}_d^2 + \tilde{i}_q^2\right)\left[\frac{\alpha_1\gamma_i^2\beta^2}{2} + \frac{\alpha_1 L_m^2}{2} + L_m\gamma_i\beta\alpha_1 + \frac{\gamma_i^2\beta^2\omega^2}{2\alpha_1}\right]$$

Considering that equation (20) combined with equation (21) gives:

$$\dot{V} < -\alpha_1\left(\tilde{\psi}_d^2 + \tilde{\psi}_q^2\right) + \left(\tilde{i}_d\tilde{\psi}_d + \tilde{i}_q\tilde{\psi}_q\right)\left[\alpha_1\gamma_i\beta + \alpha_1 L_m\right] + \left(\tilde{\psi}_d\tilde{i}_q - \tilde{\psi}_q\tilde{i}_d\right)\left[\gamma_i\beta\omega\right] - \left(\tilde{i}_d^2 + \tilde{i}_q^2\right)\left[\frac{\alpha_1\gamma_i^2\beta^2}{2} + \frac{\alpha_1 L_m^2}{2} + L_m\gamma_i\beta\alpha_1 + \frac{\gamma_i^2\beta^2\omega_{\max}^2}{2\alpha_1} + \frac{2k_p}{\alpha_1}\right]$$

and keeping in mind that we always have:

$$-\left(\tilde{i}_d^2 + \tilde{i}_q^2\right)\left[\frac{\gamma_i^2\beta^2\omega^2}{2\alpha_1}\right] \le \left(\tilde{i}_d^2 + \tilde{i}_q^2\right)\left[\frac{\gamma_i^2\beta^2\omega_{\max}^2}{2\alpha_1} + \frac{2k_p}{\alpha_1}\right]$$

and $k_p > 0$, $\alpha_1 > 0$, we have: $\dot{V} \le 0$ and the system stability with the following concepts and equations (20)-(22) is proved.

References

[1] G. Ironnides, and J.A.Tecopoouios, "Optimal efficiency slip power recovery drives," *IEEE Trans. on Energy Conv.*, Vol. 3, No. 2, pp. 342~348, 1988.

[2] J.Soltani, and A.Farrokh Payam, "A robust adaptive sliding-mode controller for slip power recovery induction machine drives," *IJECE*, Vol. 6, No. 2, pp.98~104, 2007.

[3] L. Xu and W. Cheng, "Torque and reactive power control of a doubly-fed induction machine by position sensorless scheme," *IEEE Trans. on Ind. Appl.*, Vol. 31. No. 3, pp. 636~642, 1995.

[4] M.Yamamoto, O.Motoyoshi "Active and reactive power control for doubly-fed wound rotor induction generator," *IEEE Trans. on Power Electr.*, Vol. 6, No. 4, pp. 624~629, 1991.

[5] B.Hopfensperger, D.J.Atkinson, and R.K.Lakin, "Stator-flux-oriented control of a doubly fed induction machine with and without position encoder," *IEE Proc, Electr. Power Appl.*, Vol. 147, No. 4, pp. 241~250, July 2000.

[6] S.Peresada, A.Tilli, , A.Tonielli, "Robust active-reactive power control of a doubly-fed induction generator," *in Proc.IEEE-IECON'98*, Aachen, Germany, pp. 1621~1625, Sept. 1998.

[7] S.Peresada, A.Tilli, and A.Tonielli, "Indirect stator flux-oriented output feedback control of a doubly fed induction machine," *IEEE Trans. on Contr. Sys.*, Vol. 11, No. 6, pp.875~888, Nov. 2003.

[8] Jeffery T.Spooner, Manfred Maggiore, Raul Ordonez, and Kevin M.Passino, Stable Adaptive Control and Estimation for Nonlinear Systems: Neural and Fuzzy Approximator Techniques, John Wiley and Sons, Inc, New York, 2002.

[9] A. Farrokh Payam, "Adaptive input-output feedback linearization controller for Doubly-Fed Induction Machine drive," *Serbian Journal of Electrical Engineering*, Vol. 5, No. 1, pp.139~154, May 2008.

[10] S.Peresada, A.Tilli, and A.Tonielli, "Robust output feedback control of a Doubly Fed Induction Machine," In Industrial Electronics Society, IECON '99 Proceedings, *The 25th Annual Conference of the IEEE*, Vol. 3, pp. 1348~1354, 29 Nov. ~ 3 Dec. 1999.

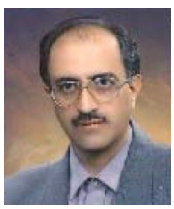

Behzad Mirzaeian Dehkordi was born in Shahr-e-kord, in the year 1966. He received the B.Sc. in Electronics Engineering from Shiraz University, Iran in 1985 and the M.Sc. and Ph.D. in Electrical Engineering from Isfahan University of Technology (IUT) in the years 1994 and 2000, respectively. In Sept. 2002, he joined the faculty of University of Isfahan, Department of Electrical Engineering as an Assistant Professor. He was a Visiting Professor in the Power Electronic Lab at Seoul National University (SNU) in South Korea from March to August 2008. His fields of interest include power electronics and drives, intelligent systems and power quality problems.

Amir Farrokh Payam received the received the B.Sc. degree in Electrical Engineering from K.N.Toosi University of Technology, Tehran, Iran in 2002 and M.Sc. degree in Electrical Engineering from Isfahan University of Technology, Isfahan, Iran in 2006. Currently he is a Ph.D. student in Electrical Engineering (Nanotechnology) in the University of Tehran, Tehran, Iran. His research interests include dynamic, modeling and control of Atomic Force Microscopes, nanomanipulation, NEMS and MEMS, applied nonlinear control, electrical drives and machines, power electronics, and applying nanotechnology to power engineering.

Mohammad Naser Hashemnia was born in Mashad, Iran, in 1984. He received the B.Sc. degree in Electrical Power Engineering from Ferdowsi University, Mashad, Iran in 2006 and the M.Sc. degree in Electrical Power Engineering from University of Tehran, Tehran, Iran in 2008. He is currently a Ph.D. student of Sharif University of Technology, Iran, where he is working on

power electronics converters. His main interests are advanced control methods of electrical drives, simulation of electric vehicles and modeling and control of power electronic converters.

Seung-Ki Sul received the B.Sc., M.Sc., and Ph.D. degrees in Electrical Engineering from Seoul National University, Seoul, Korea, in 1980, 1983, and 1986, respectively. From 1986 to 1988, he was an Associate Researcher with the Department of Electrical and Computer Engineering, University of Wisconsin, Madison. From 1988 to 1990, he was a Principal Research Engineer with Gold-Star Industrial Systems Company. Since 1991, he has been a member of the faculty of the School of Electrical Engineering, Seoul National University, where he is currently a professor. His current research interests are power electronic control of electric machines, electric/hybrid vehicle drives, and power-converter circuits.